

- [6] S. R. Batten, R. Robson, *Angew. Chem.* **1998**, *110*, 1558–1595; *Angew. Chem. Int. Ed.* **1998**, *37*, 1460–1494.
- [7] M. Eddoudi, D. B. Moler, H. Li, B. Chen, T. M. Reineke, M. O'Keeffe, O. M. Yaghi, *Acc. Chem. Res.* **2001**, *34*, 319–330.
- [8] T. M. Reineke, M. Eddaoudi, D. Moler, M. O'Keeffe, O. M. Yaghi, *J. Am. Chem. Soc.* **2000**, *122*, 4843–4844.
- [9] MCMs are readily functionalized with organic groups by post-synthetic grafting: See: M. H. Lim, C. F. Blanford, A. Stein, *J. Am. Chem. Soc.* **1997**, *119*, 4090–4091.
- [10] For studies involving metal linkers as linear bridges, see: a) K. S. Min, M. P. Suh, *Chem. Eur. J.* **2001**, *7*, 303–313; b) Y.-H. Kiang, G. B. Gardner, S. Lee, Z. Xu, E. B. Lobkovsky, *J. Am. Chem. Soc.* **1999**, *121*, 8204–8215; c) L. Carlucci, G. Ciani, D. W. V. Gudeberg, D. M. Proserpio, A. Sironi, *Chem. Commun.* **1997**, 631–632; d) M.-L. Tong, S.-L. Zheng, X.-M. Chen, *Chem. Commun.* **1999**, 561–562; e) B. F. Abrahams, B. F. Hoskins, R. Robson, *J. Am. Chem. Soc.* **1991**, *113*, 3606–3607.
- [11] M. C. T. Fyfe, J. F. Stoddart, *Acc. Chem. Res.* **1997**, *30*, 393–401.
- [12] a) A. R. Renslo, J. Rebek, Jr., *Angew. Chem.* **2000**, *112*, 3419–3421; *Angew. Chem. Int. Ed.* **2000**, *39*, 3281–3283; b) K. Choi, A. D. Hamilton, *J. Am. Chem. Soc.* **2001**, *123*, 2456–2457.
- [13] a) L. R. MacGillivray, *Cryst. Eng. Commun.* **2002**, *4*, 37–41; b) G. S. Papaefstathiou, A. J. Kipp, L. R. MacGillivray, *Chem. Commun.* **2001**, 2462–2463; c) L. R. MacGillivray, J. L. Reid, J. A. Ripmeester, *J. Am. Chem. Soc.* **2000**, *122*, 7817–7818;
- [14] G. M. J. Schmidt, *Pure Appl. Chem.* **1971**, *27*, 647–678.
- [15] A. J. Blake, N. R. Champness, S. S. M. Chung, W.-S. Li, M. Schröder, *Chem. Commun.* **1997**, 1675–1676.
- [16] For recent studies involving paddle-wheel complexes as linear bridges in extended frameworks, see: a) B. Moulton, J. Lu, M. J. Zaworotko, *J. Am. Chem. Soc.* **2001**, *123*, 9224–9225; b) F. A. Cotton, C. Lin, C. A. Murillo, *Chem. Commun.* **2001**, 11–12; c) S. R. Batten, B. F. Hoskins, B. Moubaraki, K. S. Murray, R. Robson, *Chem. Commun.* **2000**, 1095–1096; d) H. Miyasaka, C. S. Campos-Fernández, R. Clérac, K. R. Dunbar, *Angew. Chem.* **2000**, *112*, 3989–3993; *Angew. Chem. Int. Ed.* **2000**, *39*, 3831–3835; e) J. L. Wesemann, M. H. Chisholm, *Inorg. Chem.* **1997**, *36*, 3258–3267, and references therein.
- [17] a) B. Moulton, M. J. Zaworotko, *Chem. Rev.* **2001**, *101*, 1629–1658; b) P. J. Hagman, D. Hagman, J. Zubieta, *Angew. Chem.* **1999**, *111*, 2798–2848; *Angew. Chem. Int. Ed.* **1999**, *38*, 2638–2684.
- [18] 2D frameworks based on paddle-wheel complexes involving multi-topic ligands that bridge by way of axial positions have involved planar linkers (see ref. [10b–e]).
- [19] F. A. Cotton, R. A. Walton, *Multiple Bonds Between Metal Atoms*, 2nd ed., Oxford University Press, Oxford, UK, **1993**.
- [20] The smaller square cavities are comparable in size to the cavities of  $[\text{Fe}(\text{pyrazine})_2(\text{NCS})_2]$ , see: J. A. Real, G. DeMunno, M. C. Munoz, M. Julve, *Inorg. Chem.* **1991**, *30*, 2701–2704.
- [21] P. van der Sluis, A. L. Spek, *Acta. Crystallogr. Sect. A* **1990**, *46*, 194–201.
- [22] For a metal–organic cage that has molecular compartments, see: a) P. N. W. Baxter, J.-M. Lehn, A. Decian, J. Fischer, *Angew. Chem.* **1993**, *105*, 92–95; *Angew. Chem. Int. Ed. Engl.* **1993**, *32*, 89–90; b) P. N. W. Baxter, J.-M. Lehn, G. Baum, D. Fenske, *Chem. Eur. J.* **1999**, *5*, 102–112. For an organic cage that has molecular compartments, see: D. M. Rudkevich, W. Verboom, D. N. Reinhoudt, *J. Org. Chem.* **1995**, *60*, 6585–6587.
- [23] The rhombic cavity of the heated sample of **1** displays cavity dimensions  $\sim 17.1 \times 17.1 \times 5.0$  Å and corner angles of  $\sim 72^\circ$  and  $108^\circ$ . The slight deformation in shape of the cavities results in a lowering in symmetry of the unit cell to the triclinic setting.
- [24] The additional peak broadening following reintroduction of the guest precludes a single-crystal structure determination of **1**. Experiments are underway to determine the effect of guest uptake on the structure of **1** and the range of guests that may be included within the framework.
- [25] It is possible to decorate the interior of a similar IMOF with olefins (G. S. Papaefstathiou, L. R. MacGillivray, unpublished results).
- [26] Such solid-state reactivity has been referred to as latent chemical behavior, see: E. Cheung, T. Kang, J. R. Scheffer, J. Trotter, *Chem. Commun.* **2000**, 2309–2310.

- [27] We note that *trans*-1,2-bis(4-pyridyl)ethylene is photostable as a pure solid and produces a mixture of photoproducts upon UV irradiation in solution that may be separated by way of column chromatography (see: J. Vansant, S. Toppet, G. Smets, J. P. Declercq, G. Germain, *J. Org. Chem.* **1980**, *45*, 1565–1573). Therefore, **1** may be regarded as a latent MOF (see ref. [25]).
- [28] G. M. Sheldrick, SHELXL-97, Program for Refinement of Crystal Structure, University of Göttingen, Göttingen (Germany), **1997**.

## Enhanced Luminescence and Photomagnetic Properties of Surface-Modified EuO Nanocrystals\*\*

Yasuchika Hasegawa, Supitcha Thongchant, Yuji Wada, Hidekazu Tanaka, Tomoji Kawai, Takao Sakata, Hiroto Mori, and Shozo Yanagida\*

Europium(II) oxide (EuO) has localized narrow 4f orbitals that exist as the degeneracy levels between the conduction band (5d orbitals of Eu<sup>II</sup>) and the valence band (2p orbitals of O<sup>2-</sup>).<sup>[1]</sup> The 4f–5d electron transition and spin configuration of EuO lead to unique optical, magnetic, and electronic properties.<sup>[2, 3]</sup> In fact, the theoretical quantum-confinement model predicts enhanced luminescence and specific magnetic properties for nanosized Eu<sup>II</sup> semiconductors.<sup>[4, 5]</sup> Whereas the preparation of bulk EuO by thermal reduction of Eu<sub>2</sub>O<sub>3</sub> above 1000 °C was reported in 1965,<sup>[6]</sup> EuO nanocrystals were only synthesized and isolated recently. We recently prepared spindle-shaped EuO nanocrystals (average 280 nm in length and 95 nm in width) from Eu metal in liquid ammonia.<sup>[7]</sup> Here we report on the synthesis of smaller EuO nanocrystals (average diameter: 3.4 nm) by photochemical reduction of

[\*] Prof. S. Yanagida, Y. Hasegawa, S. Thongchant, Y. Wada  
Material and Life Science  
Graduate School of Engineering  
Osaka University  
2-1 Yamadaoka Suita, Osaka 565-0871 (Japan)  
Fax: (+81)6-6879-7924  
E-mail: yanagida@chem.eng.osaka-u.ac.jp

H. Tanaka, Prof. T. Kawai  
The Institute of Scientific and Industrial Research  
Osaka University  
2-1 Yamadaoka Suita, Osaka 565-0871 (Japan)  
T. Sakata, Prof. H. Mori  
Research Center for Ultra-High Voltage Electron Microscopy  
Osaka University  
2-1 Yamadaoka Suita, Osaka 565-0871 (Japan)

[\*\*] This work was supported partly by NEDO (New Energy Industrial Technology Development Organization) and Grant-in-Aid for Scientific Research No.13740397 from the ministry of Education, Science, Sports and Culture. We are grateful to Mr. S. Watae and Dr. M. Nakamoto of the Osaka City Research Center for their services in elemental analyses and ICP-AES, and Mr. Y. Yamamoto of the Institute of Scientific and Industrial Research at Osaka University for magnetic measurements. We also thank Emeritus A. Yanase at Osaka Prefecture University for helpful discussion on the magnetization of EuO, and Prof. N. Nakashima at Osaka city university for helpful discussion on the photochemical reduction of Eu<sup>III</sup>.

$\text{Eu}(\text{NO}_3)_3$  in methanol. The EuO nanocrystals have two unconventional photophysical properties: their emission quantum yield in methanol is  $49 \pm 5\%$  at 300 K, which is the highest efficiency reported for EuO, and their magnetization increases dramatically under UV irradiation at room temperature.

The EuO nanocrystals were prepared under an  $\text{N}_2$  atmosphere as described in the Experimental Section. The TEM images revealed that the sample consisted of EuO nanocrystals (Figure 1a) with an average diameter of 3.4 nm (Figure 1b). Their size distribution is much smaller than that of the recently prepared EuO nanocrystals.<sup>[7]</sup> The electron diffraction pattern (Figure 1c) of the initial nanocrystals revealed responses at 2.95, 2.43, 1.78, and 1.51 dA, corresponding to (111), (200), (220), and (222) planes of NaCl-type EuO, in agreement with those of the spindle-shaped EuO nanocrystals.<sup>[7, 8]</sup> Magnetization measurements verified the formation of  $\text{Eu}^{\text{III}}$ -free  $\text{Eu}^{\text{II}}$  oxide (EuO). Thermogravimetric/differential thermal analysis (TGA/DTA) indicated that the EuO precipitates contain 48% of organic compounds. Elemental analyses and inductively coupled plasma atomic emission spectroscopy (ICP-AES) gave empirical formulas of precipitates prepared in the absence and presence of urea of  $\text{EuH}_{6.7}\text{C}_{2.8}\text{N}_{1.2}\text{O}_{6.9}$  and  $\text{EuH}_{7.7}\text{C}_{3.3}\text{N}_{2.2}\text{O}_{6.8}$ , respectively. The empirical formula of the organic component was determined from the difference between these formulas to be  $\text{CH}_2\text{N}_2$ . As the removal of  $\text{H}_2\text{O}$  from  $\text{NH}_2\text{CONH}_2$  (urea) leaves  $\text{CH}_2\text{N}_2$ , the formation of polyurea ( $\text{NHC}(\text{O})\text{NHCH}_2$ )<sub>n</sub> on the surface of EuO was assumed, and this was confirmed by IR spectroscopy. The proposed photochemical reaction mechanism for the formation of the polyurea-modified EuO nanocrystals is shown in Figure 1d. Irradiation at the charge-transfer bands between an oxygen atom of methanol and the

$\text{Eu}^{\text{III}}$  ion of  $\text{Eu}(\text{NO}_3)_3$  induces photoreduction to give an  $\text{Eu}^{\text{II}}$  ion and  $\text{HOCH}_2^\bullet$ .<sup>[9]</sup> The radical intermediate  $\text{HOCH}_2^\bullet$  reacts with  $\text{NO}_3^-$  to give  $\text{OH}^-$  and formaldehyde. EuO is formed by the dehydrocondensation of  $\text{Eu}(\text{OH})_2$ .<sup>[10]</sup> The growth of EuO nanocrystals is coupled with the polymerization of the coordinated urea with photogenerated formaldehyde on the EuO to give polyurea-modified EuO nanocrystals.

The absorption spectrum of the polyurea-modified EuO nanocrystals in methanol is shown in Figure 2a. The band at  $\lambda = 280$  nm corresponds to the exciton band between the 4f

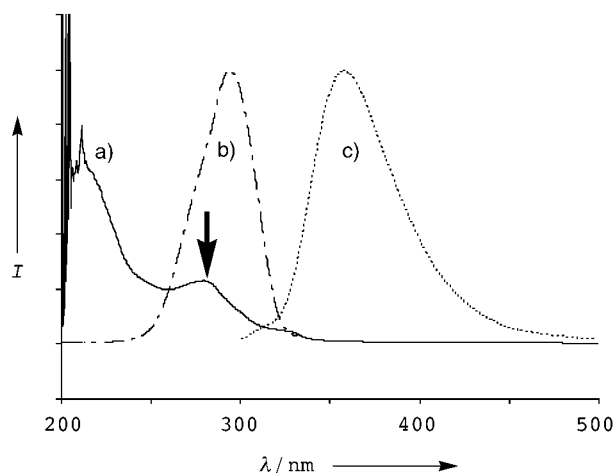


Figure 2. a) Absorption spectra of the EuO nanocrystals in methanol. The absorption below  $\lambda = 250$  nm can be assigned to polyurea and methanol, and that above  $\lambda = 250$  nm (arrow) to the exciton band of the EuO nanocrystals. b) Excitation spectrum of the EuO nanocrystals in methanol, monitored at  $\lambda = 340$  nm. c) Emission spectrum of the EuO nanocrystals in methanol (excitation at  $\lambda = 290$  nm). All spectra are corrected for detector sensitivity and lamp intensity.

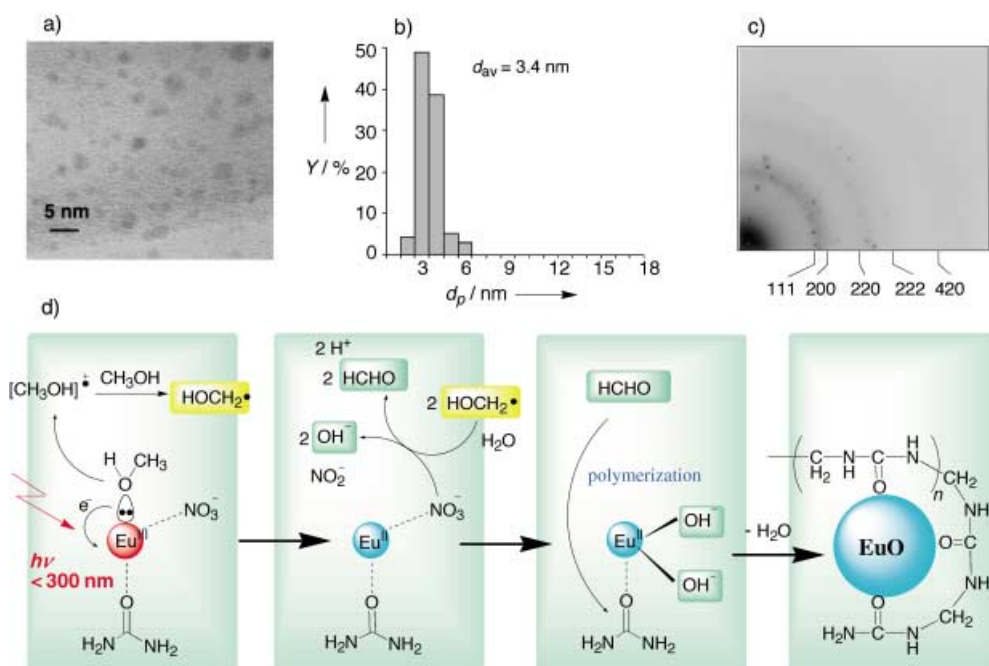


Figure 1. TEM image of the EuO nanocrystals. Images were recorded under axial illumination at approximate Scherzer focus, with a point resolution better than 0.19 nm. a) Bright-field (BF) image with weaker electron irradiation ( $2.4 \times 10^{23} \text{ e m}^{-2} \text{ s}$ , beam diameter = 2 nm). b) Size distribution of a). c) Electron diffraction pattern. d) Mechanism of the photochemical reaction.

and 5d orbitals of the EuO nanocrystals.<sup>[11]</sup> The larger Stokes shift of the exciton bands indicates that the electronic structure or spin state of EuO nanocrystals is significantly different from that of EuO bulk crystals. When the sample was irradiated at the exciton band, the emission spectrum exhibited a peak at around  $\lambda = 357$  nm. The excitation and emission spectra in methanol are shown in Figure 2b and c. The emission quantum yield of the polyurea-modified EuO in methanol was  $49 \pm 5\%$  at 300 K. Previously, the quantum efficiency of EuO single crystals was estimated to be less than 1%. Interestingly, the quantum yield of EuO nanocrystals without polyurea modification was  $5 \pm 0.5\%$  at 300 K. These results suggest that the emission quantum yields of EuO nano-

crystals depend on their surface condition. We propose that the presence of polyurea on the quantum-sized EuO surface draws the quantum-confinement effect of EuO into itself.<sup>[12]</sup>

The temperature dependence of the magnetic susceptibility  $\chi$  of the EuO nanocrystals is shown in Figure 3. From the slope of the  $T$  versus  $1/\chi$  asymptote of the EuO nanocrystals ( $3k_B/N\mu_B^2p^2$ , where  $N$  = number of atoms,  $\mu_B$  = Bohr constant,  $k_B$  = Boltzmann constant), the experimental effective number of Bohr magnetons  $p$  for the EuO nanocrystals was found to be

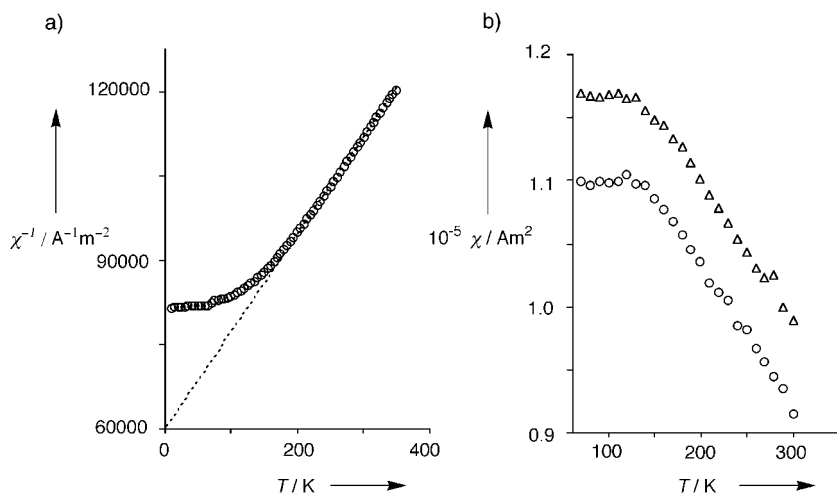


Figure 3. a) Temperature dependence of  $1/\chi$  of EuO nanocrystals under field-cooled conditions at 0.1 T in the dark. b) Temperature dependence of  $\chi$  under field-cooled conditions at 0.1 T in the dark (circles), and with irradiation (low-pressure mercury lamp,  $\lambda = 254$  nm) via optical fibers (triangles). SQUID measurements on conventional  $\text{Eu}^{\text{II}}$  compounds (e.g.,  $\text{Eu}_2\text{O}_3$ ) do not reveal enhanced magnetization under irradiation.

7.98. The theoretical effective number of Bohr magnetons for  $\text{Eu}^{\text{II}}$  ( $p = g[J(J+1)]^{1/2}$ ; total angular momentum  $J = 7/2$ , gyromagnetic ratio  $g \approx 2$ ) was calculated to be 7.94. Thus, the experimental  $p$  for EuO nanocrystals agrees well with the theoretical  $p$  for the  $4f^7$  configuration ( $\text{Eu}^{\text{II}}$ ). We also observed a dramatic increase in the magnetization of the EuO nanocrystals under UV irradiation (254 nm) at just below room temperature (triangles in Figure 3b), and this is the first report of such behavior. The  $T$  versus  $\chi$  curve of the EuO nanocrystals under irradiation paralleled that of EuO in the dark (circles in Figure 3b). This increase in magnetization under UV irradiation can be explained by a d–f exchange interaction of conducting electrons in the 5d band.<sup>[13]</sup> It is noteworthy that others recently observed photomagnetic properties of compounds only at low temperature (below 200 K).<sup>[14]</sup> The photomagnetic response of EuO nanocrystals provides experimental support for the magnetic exciton model with super-interaction between spins in the 5d band and 4f orbitals.<sup>[3]</sup>

We suggest that photo-induced increase in magnetization is attributable to the presence of an exciton band in the UV region, in accordance with the highly efficient luminescence from the polyurea-modified EuO nanocrystals. Polymers containing EuO nanocrystals are expected to be useful in applications such as plastic photo-isolators for optical fibers and photomagnetic devices.<sup>[15]</sup>

## Experimental Section

**Preparation of EuO nanocrystals:** In a quartz vessel,  $\text{Eu}(\text{NO}_3)_3$  (37.5 mm) and urea (112.5 mm) were dissolved in methanol (400 mL) under an  $\text{N}_2$  atmosphere, and the solution was irradiated with a 500-W high-pressure mercury arc lamp at 25 °C. A yellowish powder precipitated after 30 min. After 24 h of irradiation, the powder was separated by centrifugation and washed with methanol several times. High-resolution transmission electron microscopy (TEM) images of the EuO nanocrystals were obtained with a Hitachi H-9000 TEM microscope equipped with a tilting device ( $\pm 10^\circ$ ) and operating at 300 kV ( $C_s = 0.9$  mm). Absorption and emission spectra were measured on a Hitachi U-3300 spectrophotometer and Hitachi F-4500 fluorescence spectrophotometer, respectively. Emission quantum yields were determined by standard procedures by using an integrating sphere (diameter 6 cm) and quartz cells (optical path length 1 mm).<sup>[16]</sup> The magnetic susceptibility  $\chi$  of the EuO nanocrystals was measured with a superconducting quantum interface device (SQUID) magnetometer (Quantum Design, MPMS).

Received: November 7, 2001  
Revised: March 15, 2002 [Z18177]

- [1] D. E. Eastman, F. Holtzberg, S. Methfessel, *Phys. Rev. Lett.* **1969**, 23, 226–229.
- [2] P. Wachter, *Handbook on the Physics and Chemistry of Rare Earths*, 2nd Ed., North-Holland Publishing Company, **1979**, pp. 189–241.
- [3] T. Kasuya, A. Yanase, *Rev. Mod. Phys.* **1968**, 40, 684–696.
- [4] W. Chen, X. Zhang, Y. Huang, *Appl. Phys. Lett.* **2000**, 76, 2328–2330.
- [5] P. Fumagalli, A. Schirmeisen, R. J. Gambino, *J. Appl. Phys.* **1996**, 79, 5929–5931.
- [6] M. W. Shafer, *J. Appl. Phys.* **1965**, 36, 1145–1152.
- [7] S. Thongchant, Y. Hasegawa, Y. Wada, S. Yanagida, *Chem. Lett.* **2001**, 1274–1275.
- [8] The TEM image of the initial EuO was fuzzy (Figure 1 a), but all TEM BF images of EuO nanocrystals agree with those of corresponding TEM centered dark-field (CDF) images, in which the incident beam is tilted such that the scattered beam remains on-axis.
- [9] a) C. K. Jørgensen, J. S. Brinen, *Mol. Phys.* **1963**, 6, 629–631; b) M. Kusaba, N. Nakashima, W. Kawamura, Y. Izawa, C. Yamanaka, *Chem. Phys. Lett.* **1992**, 197, 136–140.
- [10] M. Izaki, T. Omi, *J. Electrochem. Soc.* **1997**, 144, L3–L5.
- [11] O. Sakai, A. Yanase, T. Kasuya, *J. Phys. Soc. Jpn.* **1977**, 42, 596–607.
- [12] Wakefield, *J. Colloid Interface Sci.* **1999**, 215, 179–182.
- [13] M. Umehara, *Phys. Rev. B* **1995**, 52, 8140–8149.
- [14] a) H. Katsu, H. Tanaka, T. Kawai, *Appl. Phys. Lett.*, **2000**, 76, 3245; b) S. Ohkoshi, K. Hashimoto, *J. Photochem. Photobiol. B* **2001**, 2, 71–88; c) G. Rombaut, M. Verelst, S. Golhane, L. Ouahab, C. Mathoniere, O. Kahn, *Inorg. Chem.* **2001**, 40, 1151–1159.
- [15] a) K. Tanaka, K. Fujita, N. Soga, J. Qui, K. Hirao, *J. Appl. Phys.* **1997**, 82, 840–844; b) T. Arakawa, T. Tanaka, G. Adachi, J. Shiokawa, *J. Lumin.* **1979**, 20, 325–327.
- [16] Y. Hasegawa, T. Ohkubo, K. Sogabe, Y. Kawamura, Y. Wada, N. Nakashima, S. Yanagida, *Angew. Chem.* **2000**, 112, 365–368; *Angew. Chem. Int. Ed.* **2000**, 39, 357–360.